# Heterocyst-specific flavodiiron protein Flv3B enables oxic diazotrophic growth of the filamentous cyanobacterium *Anabaena* sp. PCC 7120

Maria Ermakova[a], Natalia Battchikova[a], Pierre Richaud[b,c,d], Hannu Leino[a], Sergey Kosourov[a], Janne Isojärvi[a], Gilles Peltier[b,c,d], Enrique Flores[e], Laurent Cournac[b,c,d,1], Yagut Allahverdiyeva[a,2], and Eva-Mari Aro[a,2]

[a]Laboratory of Molecular Plant Biology, Department of Biochemistry, University of Turku, FI-20014, Turku, Finland; [b]Commissariat à l'Energie Atomique et aux Energies Alternatives, Institut de Biologie Environnementale et de Biotechnologie, Laboratoire de Bioénergétique et Biotechnologie des Bactéries et Microalgues, Cadarache, F-13108 Saint-Paul-lez-Durance, France; [c]Centre National de la Recherche Scientifique, Unité Mixte de Recherche 7265 Biologie Végétale et Microbiologie Environnementales; F-13108 Saint-Paul-lez-Durance, France; [d]Aix Marseille Université, Unité Mixte de Recherche 7265 Biologie Végétale et Microbiologie Environnementales, F-13284 Marseille, France; and [e]Instituto de Bioquímica Vegetal y Fotosíntesis, Consejo Superior de Investigaciones Científicas and Universidad de Sevilla, E-41092 Seville, Spain

Edited by Robert Haselkorn, The University of Chicago, Chicago, IL, and approved June 13, 2014 (received for review April 22, 2014)

**Flavodiiron proteins are known to have crucial and specific roles in photoprotection of photosystems I and II in cyanobacteria. The filamentous, heterocyst-forming cyanobacterium *Anabaena* sp. strain PCC 7120 contains, besides the four flavodiiron proteins Flv1A, Flv2, Flv3A, and Flv4 present in vegetative cells, two heterocyst-specific flavodiiron proteins, Flv1B and Flv3B. Here, we demonstrate that Flv3B is responsible for light-induced $O_2$ uptake in heterocysts, and that the absence of the Flv3B protein severely compromises the growth of filaments in oxic, but not in microoxic, conditions. It is further demonstrated that Flv3B-mediated photosynthetic $O_2$ uptake has a distinct role in heterocysts which cannot be substituted by respiratory $O_2$ uptake in the protection of nitrogenase from oxidative damage and, thus, in an efficient provision of nitrogen to filaments. In line with this conclusion, the Δ*flv3B* strain has reduced amounts of nitrogenase NifHDK subunits and shows multiple symptoms of nitrogen deficiency in the filaments. The apparent imbalance of cytosolic redox state in Δ*flv3B* heterocysts also has a pronounced influence on the amounts of different transcripts and proteins. Therefore, an $O_2$-related mechanism for control of gene expression is suggested to take place in heterocysts.**

nitrogen fixation | oxygen protection | photosynthesis

Flavodiiron proteins (FDPs, also called A-type flavoproteins) belong to a large family of proteins originally discovered and investigated in strict or facultative anaerobic bacteria, archaea, and some eukaryotic parasites (1). They have been proposed to help anaerobic species in coping with oxidative and/or nitrosative stress and to play an important role in maintaining the anaerobic metabolism. Homologs of genes encoding FDPs were later found in the genomes of oxygenic photosynthetic organisms: cyanobacteria, green algae, mosses, and lycophytes. FDPs are widespread in cyanobacteria, but have gradually disappeared in the course of higher plant evolution (2, 3). Intriguingly, the structures of the FDPs in oxygenic photosynthetic organisms are unique, because they possess an extra C-terminal flavin-reductase domain. This domain is in addition to the common core that is comprised of two redox centers, a β-lactamase–like domain including the nonheme catalytic diiron center at the N terminus and the flavin mononucleotide-containing flavodoxin-like domain at the C terminus (1, 4). Therefore, cyanobacterial-type FDPs are likely capable of donating electrons to $O_2$/NO directly from NAD(P)H. Cyanobacterial FDPs have mostly been studied in *Synechocystis* sp. strain PCC 6803 (hereafter *Synechocystis*), a unicellular non-$N_2$–fixing cyanobacterium.

The Flv2 and Flv4 proteins are present only in β-cyanobacteria and their heterodimer functions in photoprotection of photosystem (PS) II (2, 5, 6). The Flv1 and Flv3 proteins can be found in α- and β-cyanobacteria, but also in green algae, mosses, and lycophytes (2). Initial in vitro studies with recombinant Flv3 protein from *Synechocystis* provided evidence that it may function as an NAD(P)H:$O_2$ oxidoreductase reducing $O_2$ directly to water (4). Afterward, Helman et al. (7) demonstrated that the Δ*flv1* and Δ*flv3* mutants lack the light-induced $O_2$ uptake and proposed that Flv1 and Flv3 reduce molecular $O_2$ to water with NADPH produced on the acceptor side of PS I without formation of reactive oxygen species (ROS). Under certain conditions, up to 60% of electrons originating from water-splitting PS II could be forwarded to $O_2$ via Flv1 and Flv3 proteins (8). The importance of Flv1 and Flv3 for the survival of cyanobacteria was unambiguously proven only recently by application of fluctuating light to mimic the constantly changing natural illumination conditions in aquatic environments (9).

We have demonstrated the existence of two "extra" genes that represent copies of *flv1* and *flv3* in *Anabaena* sp. strain PCC 7120 (hereafter *Anabaena*), a model filamentous $N_2$-fixing, heterocyst-forming cyanobacterium. We have detected in the genome of *Anabaena* the following *flv* genes: *flv1A* (*all3891*), *flv1B* (*all0177*),

## Significance

Cyanobacterial flavodiiron proteins (FDPs) comprise a protein family with unique modular structure and photoprotective functions in an oxygenic environment. It is conceivable that FDPs have made the development of oxygenic photosynthesis possible in cyanobacteria. Here, we report the ability of specific FDPs to reduce $O_2$ directly to water in heterocyst-forming filamentous cyanobacteria, not only to support the photosynthetic machinery, but also to prevent oxidative damage of the $N_2$-fixing enzyme nitrogenase. Whilst in the ancient environment, $N_2$ fixation was secured from $O_2$ inhibition, the later increase of atmospheric $O_2$ may have initiated an important role for FDP-mediated protection of nitrogenase in maintaining the $N_2$-fixing activity of cyanobacteria.

Author contributions: M.E., N.B., Y.A., and E.-M.A. designed research; M.E., N.B., P.R., H.L., S.K., J.I., and Y.A. performed research; G.P., E.F., and L.C. contributed new reagents/analytic tools; M.E., E.F., L.C., and Y.A. analyzed data; and M.E., N.B., E.F., Y.A., and E.-M.A. wrote the paper.

The authors declare no conflict of interest.

This article is a PNAS Direct Submission.

Freely available online through the PNAS open access option.

[1]Present address: Institut de Recherche pour le Développement, Unité Mixte de Recherche Ecologie Fonctionnelle et Biogéochimie des Sols and Agro-Écosystèmes, F-34060 Montpellier, France.

[2]To whom correspondence may be addressed. Email: eva-mari.aro@utu.fi or allahve@utu.fi.

This article contains supporting information online at www.pnas.org/lookup/suppl/doi:10.1073/pnas.1407327111/-/DCSupplemental.

*flv2* (*all4444*), *flv3A* (*all3895*), *flv3B* (*all0178*), and *flv4* (*all4446*) (10). *Anabaena* forms long filaments comprised only of vegetative cells when grown in medium containing nitrate or ammonium. In the absence of combined nitrogen, some vegetative cells differentiate into heterocysts, cells with specific morphology and metabolism providing the conditions for fixation of atmospheric $N_2$ (11). Oxygenic photosynthesis in $N_2$-fixing filaments is restricted to vegetative cells. Heterocysts, in contrast, bear an extra, $O_2$-impermeable envelope with glycolipid and polysaccharide layers outside of the outer membrane, so that diffusion of gases, including $N_2$, occurs mainly through terminal pores connecting heterocysts and vegetative cells (12). Vegetative cells also supply heterocysts with energy for $N_2$ fixation, mainly in the form of sucrose, whereas heterocysts, in turn, provide the whole filament with fixed nitrogen.

An obligatory condition for the activity of nitrogenase, the key enzyme in $N_2$ fixation, is a low partial pressure of $O_2$ inside the cells (13). $O_2$ in heterocysts is thought to be eliminated immediately by respiratory complexes (12). Two clusters encoding respiratory terminal oxidases, *cox2* and *cox3*, were found to be expressed specifically in heterocysts and shown to be essential for diazotrophic growth in *Anabaena* (14, 15). Additionally, several other systems of protection against $O_2$ and ROS were recently found to be required to maintain the activity of nitrogenase or diazotrophic growth, emphasizing the ultimate importance of microoxic conditions for proper functioning of the $N_2$-fixing machinery (16–19).

Fluorescent protein tagging revealed that the duplicates of Flv1 and Flv3 are spatially segregated in the filaments of *Anabaena* (10). Flv1A and Flv3A were detected only in vegetative cells, whereas Flv1B and Flv3B were expressed only after combined nitrogen stepdown and were found exclusively in heterocysts. Flv1B and Flv3B could possibly form an operon, and the expression of Flv3B may be activated by NtcA, a global regulator of heterocyst differentiation (20, 21). Here, we investigate *Anabaena* strains lacking the heterocyst-specific flavodiiron proteins and demonstrate the existence of Flv-mediated light-induced $O_2$ uptake inside heterocysts, which is important for $N_2$ fixation and diazotrophic growth of this filamentous cyanobacterium.

## Results

**Growth Phenotype of the Mutants Lacking Heterocyst-Specific FDPs.** To clarify the roles of Flv1B and Flv3B in heterocysts, we constructed mutant strains Δ*flv1B* and Δ*flv3B*, as well as the double mutant Δ*flv1B/3B* (Fig. S1 and Table S1). In the presence of combined nitrogen, wild-type (WT) and mutant strains grew similarly (Fig. 1*A*, +N). Next, $N_2$ prototrophy of the mutants was addressed by shifting the nitrate-grown filaments to nitrate-free medium. Whereas the Δ*flv1B* mutant grew similarly to WT cells, the strains lacking Flv3B protein demonstrated approximately 50% reduced growth rate ($0.40 \pm 0.06$, $P < 0.001$) compared with WT ($0.79 \pm 0.08$) based on $OD_{750}$ measurements (Fig. 1*A*, -N). Additionally, Flv3B-depleted strains had approximately 50% lower chlorophyll (Chl) *a* and protein ratio compared with $OD_{750}$ after 4 d in $N_2$-fixing conditions (Fig. S2). To test the role of $O_2$ in slowing growth in the absence of Flv3B, the growth of the Δ*flv3B* mutant was next examined in the absence of $O_2$, i.e., while flushing with a gas mixture of 99.96% $N_2$ and 0.04% $CO_2$. The $O_2$-depleted atmosphere rescued the growth of the Δ*flv3B* mutant in $N_2$-fixing conditions similar to that of the WT (Fig. 1*B*). Furthermore, the protein amounts of the nitrogenase subunit NifH were similar in the mutant and the WT in microoxic conditions (Fig. 1*B, Inset*), which is in contrast to heavily reduced amount of NifH in the Δ*flv3B* mutant under oxic conditions (Fig. 1*A, Inset*).

To test for possible modifications in the morphology of the mutant strains, the phenotype of the filaments under $N_2$-fixing conditions in oxic environment was investigated in more detail.

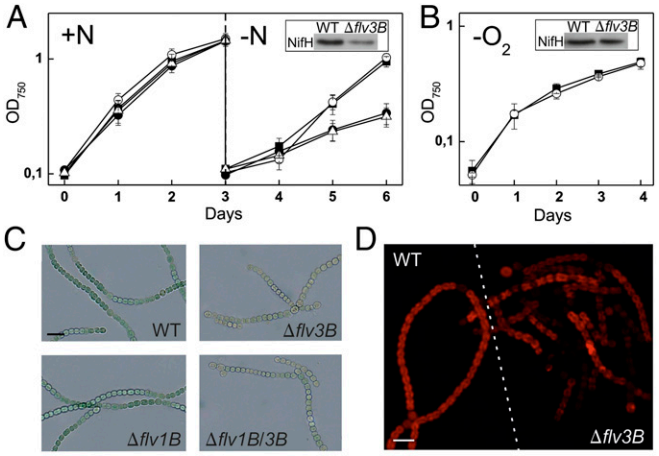


**Fig. 1.** Growth phenotype of *Anabaena* WT and the *flv* mutants. (*A*) Filaments were grown with combined N (+N) for 3 d followed by adjustment of $OD_{750}$ to 0.1 and shifting to $N_2$-fixing conditions (-N). ■, WT; mutant strains: ○, Δ*flv1B*; ●, Δ*flv3B*; △, Δ*flv1B/3B*. (*B*) Growth of the WT and Δ*flv3B* in $O_2$-depleted atmosphere after combined N stepdown: ■, WT; ○, Δ*flv3B*. (*C*) Filaments of the WT and mutants after 4 d in $N_2$-fixing conditions visualized with bright field microscopy. (*D*) Chl *a* autofluorescence of the WT and Δ*flv3B* in $N_2$-fixing conditions. (*A* and *B*) Values are mean ± SD, $n = 3$; *Insets* demonstrate amount of the NifH protein in the growth conditions. (Scale bars: 10 μm.)

Bright field microscopy revealed that single and double mutant strains lacking Flv3B consisted of only short pale-green chains of vegetative cells, typically with one or two terminal heterocysts, whereas the Δ*flv1B* strain had long filaments similar to the WT in color and heterocyst content (Fig. 1*C* and Table S2). Simultaneous monitoring of Chl *a* autofluorescence from WT and Δ*flv3B* mutant filaments confirmed that vegetative cells of the mutant contained lower amounts and uneven distribution of Chl *a* (Fig. 1*D*).

**Gas Exchange in Filaments and Heterocysts of WT and the *flv* Mutants.** We previously demonstrated that Flv1A and Flv3A proteins, located exclusively in vegetative cells, are essential for the growth of *Anabaena* under fluctuating light (9). Importantly, after nitrogen stepdown, under both the steady-state (Fig. 1*A*) and fluctuating light conditions (Fig. S3), the growth of Δ*flv1B* did not differ from that of the WT. However, the Δ*flv3B* mutant had approximately 50% lower growth rates under both light conditions compared with WT cells. This observation suggested a different role for the Flv1B and Flv3B proteins in heterocysts from that of the Flv1A and Flv3A in vegetative cells under fluctuating light conditions. The next question to address was whether Flv1B and Flv3B, like their homologs Flv1A and Flv3A, are involved in $O_2$ photoreduction. To this end, membrane inlet mass spectrometry (MIMS) was applied to monitor online gas exchange from the whole filaments incubated in $N_2$-fixing conditions. The method allows simultaneous measurement of the amount of naturally abundant $^{16}O_2$ evolved by PS II and the heavy isotope $^{18}O_2$ injected into the experimental medium before the analysis, thus making it possible to specifically distinguish the $O_2$ uptake.

As demonstrated by the MIMS gas exchange measurements (Fig. 2*A* and Table 1), illumination of the dark-adapted WT filaments with white light strongly stimulated the rate of $O_2$ uptake (69.5 μmol·[mg of Chl *a*]$^{-1}$·h$^{-1}$, hereafter rates are average; details in Table 1) compared with that in darkness (respiration, 20.3 μmol·[mg of Chl *a*]$^{-1}$·h$^{-1}$). The fraction of $O_2$ consumption during illumination, after subtraction of the dark $O_2$ uptake rate, is referred to as light-induced $O_2$ uptake (49.1 μmol·[mg of Chl *a*]$^{-1}$·h$^{-1}$). In contrast

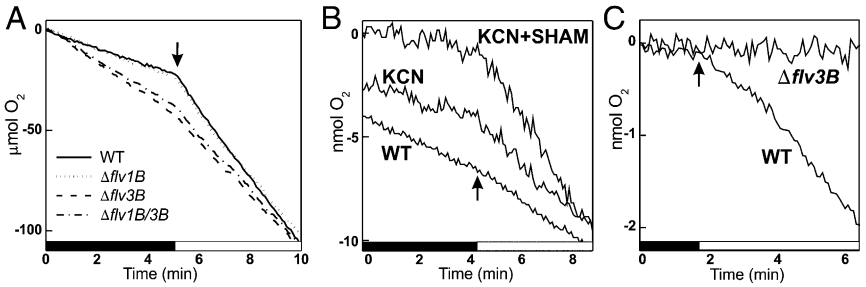


**Fig. 2.** $O_2$ uptake by $N_2$-fixing filaments and heterocysts of the WT and mutant strains. (*A*) MIMS measurements of $O_2$ consumption during the dark-to-light transition by whole filaments of the WT (solid line) and mutants: Δ*flv1B* (dotted line), Δ*flv3B* (dashed line), Δ*flv1B/3B* (dash-dot line). (*B*) $O_2$ uptake by WT heterocysts with or without inhibitors. (*C*) Light-induced $O_2$ uptake by WT and Δ*flv3B* heterocysts; dark $O_2$ uptake rates were subtracted for better legibility. Arrows indicate the beginning of illumination. Chl *a* content of samples was adjusted to 15 $\mu g \cdot ml^{-1}$.

to the WT, both Δ*flv3B* and Δ*flv1B/3B* mutants in darkness consumed more $O_2$ (32.4 and 30.4 μmol·[mg of Chl *a*]$^{-1}$·h$^{-1}$), but upon transfer to the light showed less light-induced $O_2$ uptake (21.8 and 25.4 μmol·[mg of Chl *a*]$^{-1}$·h$^{-1}$). The Δ*flv1B* mutant showed dark respiration and light-induced $O_2$ uptake rates similar to those of WT.

To specifically address the $O_2$ exchange reactions in heterocysts, we isolated heterocysts from WT and mutants and checked their ability to take up $O_2$ by using a Clark-type $O_2$ electrode. WT heterocysts demonstrated a dark-respiration rate of 3.4 μmol·[mg of Chl *a*]$^{-1}$·h$^{-1}$ and also a substantial light-induced $O_2$ uptake (2.2 μmol·[mg of Chl *a*]$^{-1}$·h$^{-1}$; Fig. 2*B*). The origin of the light-induced $O_2$ uptake was tested by supplementation with well-known inhibitors of respiratory chain components. Incubation of WT heterocysts with potassium cyanide (KCN), salicylhydroxamic acid (SHAM), or antimycin A resulted in significant inhibition of dark $O_2$ uptake, whereas the light-induced $O_2$ uptake was stimulated by the presence of these inhibitors (Fig. 2*B* and Table 1). The Δ*flv1B* heterocysts exhibited a 44% higher dark $O_2$ uptake rate than the WT, whereas the light-induced $O_2$ uptake rate was not significantly different from that in the WT. In contrast to Δ*flv1B*, the heterocysts of the Δ*flv3B* and Δ*flv1B/3B* mutants showed notably higher rates (approximately twofold) of dark respiration than the WT, whereas light-induced $O_2$ uptake was completely absent (Fig. 2*C* and Table 1).

Light-saturated photosynthesis was measured by MIMS as $O_2$ evolution from whole filaments incubated in the absence of combined nitrogen. The WT and the Δ*flv1B* mutant showed comparable rates of net $O_2$ evolution (approximately 118 μmol·[mg of Chl *a*]$^{-1}$·h$^{-1}$), whereas in the Δ*flv3B* strain, the rate was reduced by 25% (Table 1). Simultaneous analysis of $CO_2$ uptake in the presence of 10 mM $NaHCO_3$ revealed significantly lower light-induced $CO_2$ uptake in mutants lacking Flv3B compared with the WT and Δ*flv1B* (Table 1). As to the yields of PS I and PS II, the values in the Δ*flv3B* mutant under normal growth light conditions were similar to those of the WT, but upon increasing light intensity, the yields of PS I and PS II dropped more rapidly in Δ*flv3B* than in the WT (Fig. S4).

**Lack of Heterocyst-Specific Protein Flv3B Modulates the Transcriptome of Whole Filaments.** To get insights into the role of the Flv1B and Flv3B proteins in cellular metabolism, we next compared the gene expression profiles of the WT and the Δ*flv1B*, Δ*flv3B*, and Δ*flv1B/3B* mutant strains. To identify the genes with differential expression, we first isolated total RNA from whole filaments incubated under $N_2$-fixing conditions and subjected it to RNA sequencing. The genes with prominent differences in expression between the strains were then subjected to more precise transcript analysis by quantitative real-time PCR (RT-q-PCR). In Fig. 3, the RT-q-PCR results are presented as a ratio of the gene transcript abundance in each mutant over the transcript abundance in the WT.

The filaments of both mutants lacking Flv3B (the Δ*flv3B* and Δ*flv1B/3B* mutants) demonstrated similar changes in the transcript profile in comparison with the WT. Notably, we observed decreased amounts of *nifH1* mRNA (0.54 ± 0.13, hereafter data indicated is only for the Δ*flv3B* mutant), but elevated transcript abundance of *nifH2* (2.09 ± 0.68). The latter gene represents a copy of *nifH1* with nearly identical sequence but is not accompanied by copies of *nifD* and *nifK* genes. The physiological role of *nifH2* is not clear; however, it might be involved in biosynthesis of the Fe-Mo cofactor of nitrogenase (22). The transcript abundance of heterocyst-specific ferredoxin, considered to be a donor of electrons for nitrogenase (23), was also up-regulated in Flv3B-deficient mutants (*fdxH*, 1.73 ± 0.13). Importantly, genes encoding proteins involved in $O_2$ and $H_2O_2$ reduction were significantly up-regulated in the absence of Flv3B under $N_2$-fixing conditions (*coxA3*, 3.47 ± 1.58; *rbrA*, 1.98 ± 0.47;

**Table 1. The rates of $CO_2$ uptake in whole filaments and $O_2$ exchange in whole filaments and isolated heterocysts of the WT and the *flv* mutant strains**

| | Filaments | | | | | | Heterocysts | | |
|---|---|---|---|---|---|---|---|---|---|
| | | $O_2$ uptake | | | Gross $O_2$ evolution | Net $O_2$ evolution | $O_2$ uptake | | |
| Strain and inhibitors | $CO_2$ uptake | Dark | Light | Light-induced | | | Dark | Light | Light-induced |
| WT | 7.0 ± 0.3 | 20.3 ± 1.1 | 69.5 ± 0.8 | 49.1 ± 0.8 | 187.5 ± 5.5 | 118.0 ± 5.9 | 3.4 ± 0.5 | 5.6 ± 0.5 | 2.2 ± 0.7 |
| + KCN | — | — | — | — | — | — | 1.3 ± 0.4** | 5.5 ± 0.8 | 4.2 ± 0.4** |
| + KCN, SHAM | — | — | — | — | — | — | 0.7 ± 0.3** | 7.5 ± 0.5** | 6.8 ± 0.2** |
| + Antimycin A | — | — | — | — | — | — | 1.4 ± 0.6** | 5.7 ± 0.7 | 4.4 ± 0.1** |
| Δ*flv1B* | 7.5 ± 2.1 | 21.1 ± 1.6 | 58.5 ± 0.5** | 37.4 ± 2.1** | 181.5 ± 5.8 | 123.0 ± 5.0 | 4.9 ± 0.8* | 6.7 ± 0.5* | 1.8 ± 0.3 |
| Δ*flv3B* | 5.2 ± 0.3** | 32.4 ± 3.15* | 54.3 ± 2.1** | 21.8 ± 5.3** | 142.8 ± 6.8** | 88.5 ± 4.6* | 7.4 ± 0.7** | 6.5 ± 0.1* | Nd |
| Δ*flv1B/3B* | 5.1 ± 0.4** | 30.4 ± 1.4** | 55.8 ± 1.7** | 25.4 ± 3.1** | 145.5 ± 5.6** | 89.7 ± 7.2* | 6.5 ± 0.6** | 6.4 ± 0.1* | Nd |

Gas exchange rates are presented as micromoles per milligram of Chl *a* per hour. Filaments were grown in $N_2$-fixing conditions. Light-induced $O_2$ uptake was calculated by subtracting the $O_2$ uptake rate in darkness from the $O_2$ uptake rate in the light. Net $O_2$ evolution was deducted as a residual rate of gross $O_2$ evolution after subtraction of the light $O_2$ uptake rate. Mean ± SD, $n = 3$, asterisks indicate statistically significant differences with the WT (*$P < 0.05$; **$P < 0.01$). Nd, not detected.

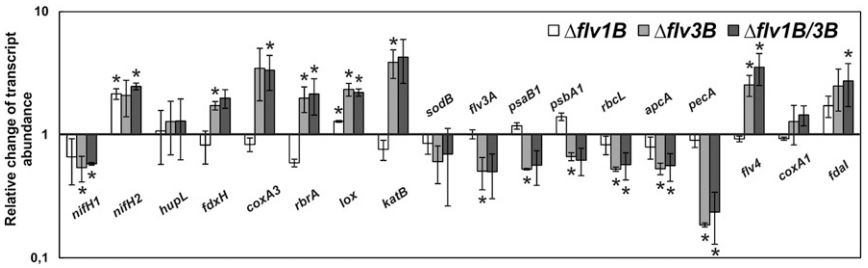


**Fig. 3.** RT-q-PCR analysis of gene expression in whole filaments of the WT and mutants incubated in the absence of combined nitrogen. The fold change of relative transcript abundance of the selected genes in mutant cells compared with the WT is shown: white bars, Δ*flv1B*; light gray bars, Δ*flv3B*; dark gray bars, Δ*flv1B/3B*. Mean ± SD, $n = 3$. Asterisks indicate statistically significant differences with the WT (*$P < 0.05$).

*lox*, 2.34 ± 0.28; *katB*, 3.88 ± 1.01). On the contrary, a specific group of photosynthesis-related genes was down-regulated (*psaB1*, 0.53 ± 0.01; *psbA1*, 0.67 ± 0.05; *rbcL*, 0.53 ± 0.02; *flv3A*, 0.51 ± 0.15), and the most prominent drop in transcript level was observed for genes encoding components of phycobilisomes (PBS): both the core (*apcA*, 0.53 ± 0.06) and the rods (*pecA*, 0.19 ± 0.01). However, the transcript amount of *flv4*, a homolog of the gene encoding the flavodiiron protein that is specifically connected to PS II and PBS in photoprotection of *Synechocystis* (6), was higher in the mutants lacking Flv3B than in WT (2.54 ± 0.49).

In the Δ*flv1B* mutant, the transcript data obtained on the level of whole $N_2$-fixing filaments demonstrated no prominent differences from that of the WT with regard to light harvesting, photosynthesis, and $N_2$ fixation-related genes. However, *nifH1* gene was down-regulated compared with the WT (0.66 ± 0.26), whereas expression of the *nifH2* gene was higher (2.15 ± 0.21).

**Protein Composition of Heterocyst-Specific *flv* Mutants.** To track changes on the protein level, we compared Δ*flv1B*, Δ*flv3B*, and WT, using both the whole filaments incubated in the absence of combined nitrogen and heterocyst-enriched cell fractions. For protein comparison, the differential gel electrophoresis (DIGE) approach was taken to identify differentially abundant proteins (Fig. S5). The difference in expression of proteins between Δ*flv3B* and WT is hereafter shown as a ratio of the relative protein amount in the mutant compared with the WT; a full list of proteins and ratio values are presented in Table S3. Whole filaments of the Δ*flv3B* mutant completely lacked the PecA and PecC proteins, which are the phycoerythrocyanin component of PBS rods and its linker protein, respectively. The down-regulated proteins included the large subunit of ribulose bisphosphate carboxylase (RbcL, 0.6 ± 0.1), fructose bisphosphate aldolase (Fda II, 0.7 ± 0.1), glyceraldehyde-3-phosphate dehydrogenase (Gap2, 0.6 ± 0.0), D-fructose-1,6-bisphosphatase class 2/sedoheptulose-1,7-bisphosphatase (GlpX, 0.7 ± 0.0), thioredoxin reductase (TrxB, 0.6 ± 0.1), and several proteins involved in various biosynthesis pathways: sulfolipid biosynthesis protein (Alr1744), ketol-acid reductoisomerase (IlvC), protochlorophyllide oxidoreductase (Por), and glucose-1-phosphate adenylyltransferase (GlgC).

In the heterocyst fraction of Δ*flv3B*, the most prominent decrease was observed for subunits of nitrogenase (NifH, 0.5 ± 0.1; NifD, 0.5 ± 0.1; NifK, 0.6 ± 0.0) and uptake hydrogenase (HupL, 0.3 ± 0.0). Further, down-regulation was recorded for GlpX (0.7 ± 0.1), 6-phosphogluconate dehydrogenase (6-PGD, 0.5 ± 0.1), aconitate hydratase (AcnB), TrxB, enzymes of Chl biosynthesis geranylgeranyl hydrogenase (ChlP) and Por, and several other proteins. As expected, heterocysts lacked Flv3B protein, but Flv1B was detected in a higher amount than in WT (3.3 ± 0.5). Among other up-regulated proteins, we identified Fda I (1.9 ± 0.1), transaldolase (Tal, 1.5 ± 0.0), succinate-semialdehyde dehydrogenase (1.8 ± 0.3), and alanine dehydrogenase (Ald, 3.5 ± 0.4). Likewise, two porins, Alr0834 and All4499, possibly involved in cell wall remodeling of heterocysts (11), were found in higher amounts in the Δ*flv3B* mutant.

In contrast to the Δ*flv3B* mutant, the Δ*flv1B* strain, which did not differ much in growth characteristics from the WT (Fig. 1*A*), demonstrated only subtle changes in protein amounts in both heterocysts and whole $N_2$-fixing filaments (Fig. S5 and Table S4). However, several proteins up-regulated in whole filaments of the Δ*flv1B* mutant were Fda I, Fda II, and Gap2. PecA and 6-PGD showed decreased amounts in Δ*flv1B* filaments. In heterocysts of the Δ*flv1B* mutant, Flv1B was absent, as expected, but the amount of Flv3B was similar to that in the WT. Decreased amounts of HupL, TrxB, and 6-PGD were also observed in Δ*flv1B* heterocysts, but the mutation did not have an effect on protein amounts of the nitrogenase subunits.

**Nitrogenase Activity of the Mutant Strains.** In oxic acetylene reduction assays, the WT showed a nitrogenase activity rate of 19.6 ± 0.2 μmol·[mg of Chl]$^{-1}$·h$^{-1}$. All mutants studied had a significantly lower nitrogenase activity compared with the WT: 10.3 ± 4.1, 11.1 ± 1.6, and 8.9 ± 1.5 μmol·[mg of Chl]$^{-1}$·h$^{-1}$ by Δ*flv1B*, Δ*flv3B*, and the double mutant, respectively (mean ± SD, $n = 3$, $P < 0.05$).

## Discussion

**Flavodiiron Protein Flv3B Is Responsible for Light-Induced $O_2$ Uptake in Heterocysts.** $N_2$ fixation in heterocysts is an energetically expensive process that requires large amounts of reducing equivalents and ATP, which are ultimately provided by photosynthesis occurring in vegetative cells during illumination. It is conceivable that the efficient diffusion of PS II-generated $O_2$ into the heterocyst occurs mainly through terminal pores according to the concentration gradient (12).

Besides respiratory $O_2$ uptake pathways, this extra $O_2$ might be taken in charge by the PS I-driven light-induced $O_2$ quenching system in heterocysts (13). Such light-induced $O_2$ uptake of unknown nature has been reported and discussed in respect to protection of the nitrogenase activity against oxidative damage (24, 25). Here, we demonstrate $O_2$ uptake by isolated heterocysts in darkness (Fig. 2*B*), i.e., respiratory activity that has been postulated as a means to decrease partial $O_2$ pressure in heterocysts (12). We also show that $O_2$ uptake increases 1.6-fold in WT heterocysts upon a dark-to-light transition. Whereas dark $O_2$ uptake is inhibited by respiratory electron transfer inhibitors, light-induced $O_2$ uptake remains unaffected (Fig. 2*B*). However, light-induced $O_2$ uptake is completely eliminated by disruption of the *flv3B* gene (Fig. 2*C*). This unambiguously indicates that the flavodiiron protein Flv3B is responsible for $O_2$ photoreduction in heterocysts.

Flv3B-dependent $O_2$ reduction in heterocysts appears to be crucial for growth and photosynthesis of *Anabaena* filaments upon removal of combined nitrogen (Fig. 1). Only the Δ*flv3B* mutant, but not Δ*flv1B*, has lost the capability for light-induced $O_2$ uptake in heterocysts. In line with this observation, the presence of the Flv1B protein in Δ*flv3B* heterocysts did not rescue the severe Δ*flv3B* phenotype. We suggested earlier that flavodiiron proteins in cyanobacteria function as heterodimers, but in the case of heterocyst-specific FDPs, Flv3B is clearly capable of functioning independently. Therefore, the function of Flv1B remains unclear.

Extra FDP-coding genes are present in genomes of all heterocyst-forming cyanobacteria sequenced to date (10). Thus, Flv3B seems to have a unique role in $O_2$ quenching in heterocysts. It is dispensable for $N_2$ fixation-dependent growth when *Anabaena* is incubated under microoxic conditions (Fig. 1*B*). However, its absence leads to strong growth impairment in oxic conditions, even if dark $O_2$ uptake appears stimulated in mutants. Therefore, Flv3B function cannot be replaced by up-regulation of common respiratory pathways, which likewise consume $O_2$. Although terminal oxidases are concentrated in the membranes near to cell junctions (26), Flv3B protein is equally distributed across the heterocysts (10), likely following the localization of the nitrogenase enzyme. By eliminating molecular $O_2$, Flv3B may participate in the control of the redox status of the cytosol and provide appropriate conditions for the function of nitrogenase, and probably many other enzymes, under illumination.

**Possible Donors of Electrons for Flv3B.** Identification of Flv3B as a responsible protein for light-induced $O_2$ uptake in heterocysts raises a question about its electron donor. NADPH and NADH were both proven to donate electrons to *Synechocystis* Flv3 in vitro (4). However, the electron donor might also be ferredoxin, because FdxI, one of ferredoxins of *Chlamydomonas reinhardtii*, was recently found to interact with Flv3, a homolog of cyanobacterial-like flavodiiron proteins (27). Current knowledge of heterocyst-specific metabolism does not allow us to make a direct distinction between possible electron donors to Flv3B. Nevertheless, it is known that heterocysts harbor only the "short" form of ferredoxin:NADPH oxidoreductase (FNR), i.e., the form that lacks the PBS-binding domain and is active in oxidation of NADPH, making it unlikely that $NADP^+$ is reduced on the reducing side of PS I in heterocysts (28). Therefore, it is conceivable that both NADPH and NADH are produced by glycolysis and oxidative pentose phosphate pathway (OPPP) equally in darkness and under the light. As to ferredoxin serving as an electron donor to Flv3B, two heterocyst-specific ferredoxins are known in *Anabaena*. The *fdxN* gene within the main *nif* gene cluster encodes a "bacterial-type" ferredoxin (29). Although its role remains unclear, the disruption of *fdxN* did not affect the diazotrophic growth of *Anabaena variabilis* (30). Another ferredoxin, encoded by *fdxH*, has been shown to function as a physical donor of electrons to nitrogenase in vitro and was suggested to play a role as a common pool where reducing equivalents from different reactions are collected to be tunneled further to $N_2$ fixation (23). FdxH takes electrons from PS I in the light but can also be reduced by FNR in darkness with the use of NADPH produced in OPPP.

We suggest that illumination modifies the redox status of heterocysts and activates the Flv3B-mediated electron transfer from the reducing side of PS I, likely from FdxH, to $O_2$. In this case, Flv3B uses light-driven electrons originating from reductants provided by vegetative cells. Based on the model structure of the Flv2/Flv4 heterodimer (5), arrangement of an Flv3B homodimer positions two cysteine residues in close proximity on the surface of the protein, where they may be available for redox regulation. Nevertheless, a possibility of a so far unknown electron carrier for reducing Flv3B cannot be excluded.

**Flv3B-Mediated Protection of Nitrogenase Ensures Sufficient Supply of Filaments with Nitrogen.** Although *flv* mutants demonstrated approximately 50% decreased nitrogenase activity compared with WT in acetylene reduction assay, it is conceivable that the maximum capacity of enzyme activity is not reached in native conditions. In the Δ*flv1B* mutant, a lower nitrogenase activity does not reduce the growth of filaments. Mutants lacking Flv3B have a similar potential for $N_2$ fixation; however, in practice, the absence of light-induced $O_2$ uptake in heterocysts results in an insufficient supply of amino acids to filaments. This notion is indicated by the multiple symptoms of nitrogen starvation in filaments of the Δ*flv3B* mutant. Most prominent is the impaired growth and modified shape of the mutant filaments (Fig. 1 *A* and *C*), as well as lower $CO_2$ uptake and gross $O_2$ evolution rates at saturating light intensity (Table 1). The decreased levels of gas exchange indicate programmed down-regulation of photosynthesis and carbon assimilation activities in response to nitrogen starvation. At the gene expression level, these symptoms are seen as a scarcity of transcripts and, consequently, of proteins from PBS-coding genes, down-regulation of photosynthesis-related genes, and reduced amounts of proteins involved in Chl synthesis (ChlP and Por), the Calvin cycle (RbcL, Fda II, and Gap2), and sugar anabolism (GlpX and GlgC). These defects are typically connected to nitrogen starvation (31). The elevated dark $O_2$ uptake rate by filaments of the Δ*flv3B* mutant might also indicate a decreased N:C ratio, because nitrogen starvation causes an accumulation of succinate, fumarate, and malate in the citric acid cycle (TCA), and respiratory activity helps to dissipate the excess carbon (32).

**Role of Flv3B in Regulation of Expression of Genes and Proteins.** The *flv3B* gene might be classified as a "late heterocyst differentiation gene" because it is actively transcribed in fully formed heterocysts, similar to the *nif* genes (33). Therefore, the lack of Flv3B does not have an effect on the formation of heterocysts, but instead modifies the fitness of the cells. The decreased amounts of NifHDK protein subunits of nitrogenase and the HupL subunit of uptake hydrogenase in the Δ*flv3B* mutant is in line with elevated $O_2$ levels in Δ*flv3B* heterocysts upon illumination. Both enzymes are known to be extremely sensitive to $O_2$ because oxidation of iron centers is expected to trigger degradation of the proteins. However, in the case of nitrogenase subunits, the lower protein amount might simply result from the transcript scarcity.

Control of gene expression in heterocysts under steady-state conditions has not yet been thoroughly investigated. However, it is conceivable that once nitrogenase is active, nitrogen deprivation is no more an ultimate driving factor for modulating nitrogenase gene expression, and other mechanisms might take over. Unlike the direct transcriptional regulation by $O_2$ of the nitrogenase genes in nonphotosynthetic diazotrophs (34), the expression of *nifHDK* in *Anabaena* has been considered to be mainly subject to developmental control (35). In line with this idea, the WT level of *nif* gene expression was observed in developing heterocysts of a double *cox2 cox3* mutant of *Anabaena* (15) despite apparently elevated $O_2$ partial pressure. However, we cannot exclude that regulation of gene expression in heterocysts is carried out by $O_2$ indirectly, through subsequent $O_2$ interactions in a cell. Indeed, $O_2$-induced modification of cytosolic redox status or degradation products of the nitrogenase protein might trigger a signaling cascade resulting in strong transcriptional changes of genes encoding nitrogenase, $O_2$ scavenging enzymes, and other proteins. In accordance with this notion, up-regulation of *coxA3*, part of an operon encoding a heterocyst-specific terminal oxidase; *lox*, which encodes lactate oxidase that is thought to reduce $O_2$; and genes encoding rubrerythrin and Mn catalase, both reducing $H_2O_2$, were found in the mutants lacking Flv3B (Fig. 3). Lactate oxidase and rubrerythrin have been shown to be important for diazotrophic growth and nitrogenase activity, respectively (17, 18).

Our data also demonstrate that Flv3B is crucial for protein composition in *Anabaena*. Many proteins were present in different amounts in the Δ*flv3B* mutant compared with WT, especially in the heterocyst-enriched fraction. The profound adjustment of protein composition likely allows the mutant to partially overcome the severe effects of the mutation and maintain a level of nitrogenase activity. Our findings reiterate the importance of mechanisms for gene and protein regulation in mature heterocysts that are yet to be investigated.

**Concluding Remarks.** Understanding the ultimate importance of flavodiiron proteins for the well-being of cyanobacteria has emerged

only during the past few years. It is highly likely that evolution of FDPs made the appearance of oxygenic photosynthesis possible by providing protection at multiple sites: the Flv2/Flv4 heterodimer protects against photoinhibition of PS II, whereas Flv1(A) and Flv3(A) prevent the photodamage of PS I. Here, we demonstrate that a heterocyst-specific flavodiiron protein Flv3B is crucial for elimination of $O_2$ in illuminated heterocysts, thereby contributing to solve the long-lasting problem of $O_2$ protection of nitrogenase in the light. The ability of FDPs to transfer light-driven electrons from downstream of PS I directly to $O_2$ can be used in heterocysts to prevent oxidative damage of the $N_2$-fixing machinery and to create appropriate redox conditions for heterocyst metabolism.

## Materials and Methods

*Anabaena* sp. (also known as *Nostoc* sp.) strain PCC 7120 and mutant strains were grown in BG-11o medium (lacking combined nitrogen) buffered with 10 mM TES–KOH (pH 8.2) in the presence of 3% (vol/vol) $CO_2$ under gentle agitation at 30 °C and constant illumination of 50 μmol photons·$m^{-2}$·$s^{-1}$. Where indicated, the cells were cultivated in BG-11 medium containing 17.6 mM $NaNO_3$. The cells at the exponential growth phase (about $OD_{750} = 1$) were harvested, resuspended in a fresh medium, and subjected to the activity measurements or to RNA and protein analyses. The growth rate constants were determined as tangents of growth curves plotted in logarithmic scale. To create microoxic conditions, the cultures were grown under continuous bubbling with gas mixture containing 99.96% $N_2$ and 0.04% $CO_2$. Filaments were visualized with a Zeiss Axiovert 200M microscope. Chl *a* was excited with a 488-nm argon ion laser, and fluorescence was collected across 680–720 nm.

The construction of the Δ*flv1B*, Δ*flv3B*, and Δ*flv1B/3B* mutant strains of *Anabaena* by triparental mating, isolation of heterocysts, nitrogenase activity assay, immunodetection, and DIGE are described in detail in *SI Materials and Methods*. Isolation of total RNA from whole filaments of WT and mutant strains and RT-q-PCR analysis were performed as described (10); the list of primers is provided in Table S1. Strand-specific transcriptome sequencing was performed by Illumina HiSeq2000 (BGI Tech Solutions, Co., Ltd.).

$O_2$ (mass 32), $^{18}O_2$ (mass 36), and $CO_2$ exchange were monitored by MIMS as described earlier (8). Actinic light at the intensity of 600 μmol photons·$m^{-2}$·$s^{-1}$ was applied by a LED-powered fiber optic illuminator (PerkinElmer Life Sciences) when needed. $O_2$ consumption by isolated heterocysts was measured with a Clark type oxygen electrode (DW1, Hansatech) in darkness and at a saturating light intensity of 400 μmol photons·$m^{-2}$·$s^{-1}$. The final concentration of inhibitors used was 1 mM KCN, 10 mM SHAM, and 10 μM Antimycin A. Chl *a* fluorescence and P700 oxidoreduction were recorded by DUAL-PAM-100 (Walz) upon application of saturating pulses (4,000 μmol photons·$m^{-2}$·$s^{-1}$, 300 ms) at stepwise increments of actinic light intensities duration of 30 s.

**ACKNOWLEDGMENTS.** We thank Cell Imaging Core and Proteomics Facility of Turku Centre for Biotechnology. Research was financially supported by the Academy of Finland Projects 118637, 271832, and 273870 (to E.-M.A.), Kone Foundation (Y.A.), and Varsinais-Suomi Cultural Foundation regional fund (M.E.). Support was provided by the HélioBiotec platform, funded by the European Union (European Regional Development Fund), the Région Provence Alpes Côte d'Azur, the French Ministry of Research, and the "Commissariat à l'Energie Atomique et aux Energies Alternatives."

1. Vicente JB, Justino MC, Gonçalves VL, Saraiva LM, Teixeira M (2008) Biochemical, spectroscopic, and thermodynamic properties of flavodiiron proteins. *Methods Enzymol* 437:21–45.
2. Zhang P, Allahverdiyeva Y, Eisenhut M, Aro EM (2009) Flavodiiron proteins in oxygenic photosynthetic organisms: Photoprotection of photosystem II by Flv2 and Flv4 in Synechocystis sp. PCC 6803. *PLoS ONE* 4(4):e5331.
3. Peltier G, Tolleter D, Billon E, Cournac L (2010) Auxiliary electron transport pathways in chloroplasts of microalgae. *Photosynth Res* 106(1-2):19–31.
4. Vicente JB, Gomes CM, Wasserfallen A, Teixeira M (2002) Module fusion in an A-type flavoprotein from the cyanobacterium Synechocystis condenses a multiple-component pathway in a single polypeptide chain. *Biochem Biophys Res Commun* 294(1): 82–87.
5. Zhang P, et al. (2012) Operon flv4-flv2 provides cyanobacterial photosystem II with flexibility of electron transfer. *Plant Cell* 24(5):1952–1971.
6. Bersanini L, et al. (2014) Flavodiiron protein Flv2/Flv4-related photoprotective mechanism dissipates excitation pressure of PSII in cooperation with phycobilisomes in Cyanobacteria. *Plant Physiol* 164(2):805–818.
7. Helman Y, et al. (2003) Genes encoding A-type flavoproteins are essential for photoreduction of $O_2$ in cyanobacteria. *Curr Biol* 13(3):230–235.
8. Allahverdiyeva Y, et al. (2011) Interplay between flavodiiron proteins and photorespiration in Synechocystis sp. PCC 6803. *J Biol Chem* 286(27):24007–24014.
9. Allahverdiyeva Y, et al. (2013) Flavodiiron proteins Flv1 and Flv3 enable cyanobacterial growth and photosynthesis under fluctuating light. *Proc Natl Acad Sci USA* 110(10):4111–4116.
10. Ermakova M, Battchikova N, Allahverdiyeva Y, Aro EM (2013) Novel heterocyst-specific flavodiiron proteins in Anabaena sp. PCC 7120. *FEBS Lett* 587(1):82–87.
11. Kumar K, Mella-Herrera RA, Golden JW (2010) Cyanobacterial heterocysts. *Cold Spring Harb Perspect Biol* 2(4):a000315.
12. Walsby AE (2007) Cyanobacterial heterocysts: Terminal pores proposed as sites of gas exchange. *Trends Microbiol* 15(8):340–349.
13. Böthe H, Schmitz O, Yates MG, Newton WE (2010) Nitrogen fixation and hydrogen metabolism in cyanobacteria. *Microbiol Mol Biol Rev* 74(4):529–551.
14. Jones KM, Haselkorn R (2002) Newly identified cytochrome c oxidase operon in the nitrogen-fixing cyanobacterium Anabaena sp. strain PCC 7120 specifically induced in heterocysts. *J Bacteriol* 184(9):2491–2499.
15. Valladares A, Maldener I, Muro-Pastor AM, Flores E, Herrero A (2007) Heterocyst development and diazotrophic metabolism in terminal respiratory oxidase mutants of the cyanobacterium Anabaena sp. strain PCC 7120. *J Bacteriol* 189(12):4425–4430.
16. Zhao W, Guo Q, Zhao J (2007) A membrane-associated Mn-superoxide dismutase protects the photosynthetic apparatus and nitrogenase from oxidative damage in the Cyanobacterium Anabaena sp. PCC 7120. *Plant Cell Physiol* 48(4):563–572.
17. Zhao W, Ye Z, Zhao J (2007) RbrA, a cyanobacterial rubrerythrin, functions as a FNR-dependent peroxidase in heterocysts in protection of nitrogenase from damage by hydrogen peroxide in Anabaena sp. PCC 7120. *Mol Microbiol* 66(5):1219–1230.
18. Hackenberg C, et al. (2011) Cyanobacterial lactate oxidases serve as essential partners in $N_2$ fixation and evolved into photorespiratory glycolate oxidases in plants. *Plant Cell* 23(8):2978–2990.
19. Ekman M, Sandh G, Nenninger A, Oliveira P, Stensjö K (2014) Cellular and functional specificity among ferritin-like proteins in the multicellular cyanobacterium Nostoc punctiforme. *Environ Microbiol* 16(3):829–844.
20. Mitschke J, Vioque A, Haas F, Hess WR, Muro-Pastor AM (2011) Dynamics of transcriptional start site selection during nitrogen stress-induced cell differentiation in Anabaena sp. PCC7120. *Proc Natl Acad Sci USA* 108(50):20130–20135.
21. Picossi S, Flores E, Herrero A (2014) ChIP analysis unravels an exceptionally wide distribution of DNA binding sites for the NtcA transcription factor in a heterocyst-forming cyanobacterium. *BMC Genomics* 15:22.
22. Rangaraj P, Ludden PW (2002) Accumulation of $^{99}$Mo-containing iron-molybdenum cofactor precursors of nitrogenase on NifNE, NifH, and NifX of Azotobacter vinelandii. *J Biol Chem* 277(42):40106–40111.
23. Böhme H, Haselkorn R (1988) Molecular cloning and nucleotide sequence analysis of the gene coding for heterocyst ferredoxin from the cyanobacterium Anabaena sp. strain PCC 7120. *Mol Gen Genet* 214(2):278–285.
24. Peterson RB, Burris RH (1976) Properties of heterocysts isolated with colloidal silica. *Arch Microbiol* 108(1):35–40.
25. Milligan AJ, et al. (2007) Light-dependent oxygen consumption in nitrogen-fixing cyanobacteria plays a key role in nitrogenase protection. *J Phycol* 43(5):845–852.
26. Murry MA, Olafsen AG, Benemann JR (1981) Oxidation of diaminobenzidine in the heterocysts of Anabaena cylindrica. *Curr Microbiol* 6(4):201–206.
27. Peden EA, et al. (2013) Identification of global ferredoxin interaction networks in Chlamydomonas reinhardtii. *J Biol Chem* 288(49):35192–35209.
28. Omairi-Nasser A, Galmozzi CV, Latifi A, Muro-Pastor MI, Ajlani G (2014) NtcA is responsible for accumulation of the small isoform of ferredoxin:NADP oxidoreductase. *Microbiology* 160(Pt 4):789–794.
29. Mulligan ME, Haselkorn R (1989) Nitrogen fixation (nif) genes of the cyanobacterium Anabaena species strain PCC 7120. The nifB-fdxN-nifS-nifU operon. *J Biol Chem* 264(32):19200–19207.
30. Masepohl B, Görlitz K, Monnerjahn U, Moslerand B, Böhme H (1997) The ferredoxin-encoding fdxN gene of the filamentous cyanobacterium Anabaena variabilis ATCC 29413 is not essential for nitrogen fixation. *New Phytol* 136(3):419–423.
31. Krasikov V, Aguirre von Wobeser E, Dekker HL, Huisman J, Matthijs HC (2012) Time-series resolution of gradual nitrogen starvation and its impact on photosynthesis in the cyanobacterium Synechocystis PCC 6803. *Physiol Plant* 145(3):426–439.
32. Osanai T, et al. (2014) Capillary electrophoresis-mass spectrometry reveals the distribution of carbon metabolites during nitrogen starvation in Synechocystis sp. PCC 6803. *Environ Microbiol* 16(2):512–524.
33. Flaherty BL, Van Nieuwerburgh F, Head SR, Golden JW (2011) Directional RNA deep sequencing sheds new light on the transcriptional response of Anabaena sp. strain PCC 7120 to combined-nitrogen deprivation. *BMC Genomics* 12:332.
34. Martínez-Argudo I, Little R, Shearer N, Johnson P, Dixon R (2005) Nitrogen fixation: Key genetic regulatory mechanisms. *Biochem Soc Trans* 33(Pt 1):152–156.
35. Elhai J, Wolk CP (1990) Developmental regulation and spatial pattern of expression of the structural genes for nitrogenase in the cyanobacterium Anabaena. *EMBO J* 9(10): 3379–3388.